International Journal of
INTELLIGENT SYSTEMS AND APPLICATIONS IN ENGINEERING
ISSN:2147-6799 www.ijisae.org Original Research Paper

# Optimized Deep Learning Model for Predicting Brain Tumors

**Narayan B. Vikhe[1*], Manish Shrivastava[2]**

**Submitted**: 07/03/2024 **Revised**: 22/04/2024 **Accepted**: 01/05/2024

**Abstract:** Brain tumors, which grow unexpectedly and can cause brain damage, are diagnosed using magnetic resonance imaging (MRI) methods. However, these methods can be time-consuming and unreliable. deep learning models have been developed to predict brain cancers using MRI scans. The research developed a white headed timber optimization based deep CNN model, which uses the Brats 2019 and 2020 datasets as input. The model passes through pre-processing, segmentation, feature extraction, and fine-tuning using white-headed-timber based optimization. the training percentage (TP) and k-fold were consider using database 1, the accuracy (acc), sensitivity (sen), and specificity (spe) for D1 and D2 were achieved at 98.37%, 98.31%, and 98.88% correspondingly. For d2, the values were 97.74%, 98.53%, and 99.15%. Similar results were obtained during k-fold 10 for d1 98.37%, 98.31%, and 98.88%. d2 are 97.74%, 98.53%, and 99.15%. The research aims to develop a WHT-based deep CNN for predicting brain cancers using MRI scans.

***Keywords:*** *Brain tumor prediction, deep CNN, WHT, MRI image, segmentation*

## 1. Introduction

The grid search optimization method allows for the automatic identification of all of the critical hyper parameters in CNN models [1]. The skull is the most complex part of the human body since it contains the brain. The brain, an essential component of the human body, is responsible for control and decision-making. This area must be protected from damage and disease because it serves as the nervous system's control center [2]. A lot of study has been done utilizing CNN to recognize many kinds of brain cancers. To categorize the different types of brain tumors, one such study used 3064 T1-weighted contrast-enhanced MRI scans. For the purpose of choosing the best features, two evolutionary methods were used: genetic algorithm and simulated annealing (SA-GA). This approach performs more effectively and is more efficient when tested on the BRATS2015 and ISLES2015 datasets [3]. The CNN-based strategy aimed to classify brain cancers in multiple categories for early diagnosis. With enough medical images, CNN models can be trained and tested. Brain MR is accurately classified as glioma, meningioma, pituitary, normal brain, and metastatic [4].Most brain tumor's causes are still a mystery. A complete medical record, however, helps assess the probability or cause of its development [5]. According to its characteristics and competing therapies, a tumor is categorized into numerous kinds.

Tumors are the unchecked proliferation of malignant cells in any organ. One of the most dangerous and serious types of tumors is the brain tumor [6].

As a result, the categorization and detection phases of tumor image processing frequently employ sophisticated digitalized image processing algorithms [7].

The research aims to develop a WHT-based deep CNN for predicting brain cancers using MRI scans. The input consists of d1 and d2, which undergo pre-processing, segmentation, feature extraction, and classification. The optimized deep CNN classifier classifies and labels clusters of pixels or vectors within the image, ensuring accurate prediction of brain cancers.

- ***White headed timber optimization:*** Grey wolf and bald eagle optimization are combined to create WHT. Grey wolves face time complexities due to group hunting, while white head eagles swoop prey immediately, reducing complexity. This swooping strategy allows for position updates for grey wolves.
- ***WHO based deep CNN:*** Deep CNN is effectively tuned utilizing the white headed timber optimization and accurately predicts brain tumors, which helps to solve the over fitting issue.

## 2. Methodology

The research aims to use a WHT-based deep CNN model to predict brain cancers using MRI scans. The three primary research steps include pre-processing, segmentation, and classification. The MRI images are inputted from d1 and d2 datasets, processed through pre-processing, segmentation, feature extraction, and classification. The extracted features are then passed

[1*]*Phd Scholar, Computer Science Engineering, Vivekananda Global University, Jaipur, India*
*aryanvikhe007@gmail.com*
[2] *Professor, Computer Science Engineering, Vivekananda Global University, Jaipur, India.*
**** Corresponding Author**: Narayan B. Vikhe*
**Scholar, Computer Science Engineering, Vivekananda Global University, Jaipur, India*

through an optimized deep CNN classifier to classify and label clusters of pixels or vectors within the image.

The hyper parameters are then fine-tuned by combining white-headed-timber based optimisation, which makes use of the Bald eagle Optimization [8] and Grey wolf Optimization [9]. The proposed WHT based deep CNN, which classifies the stage of brain cancer based on the extracted characteristics, is used in the most recent instance to predict and categorize the brain tumour-affected area utilising test data in terms of normal, benign, and maligned.

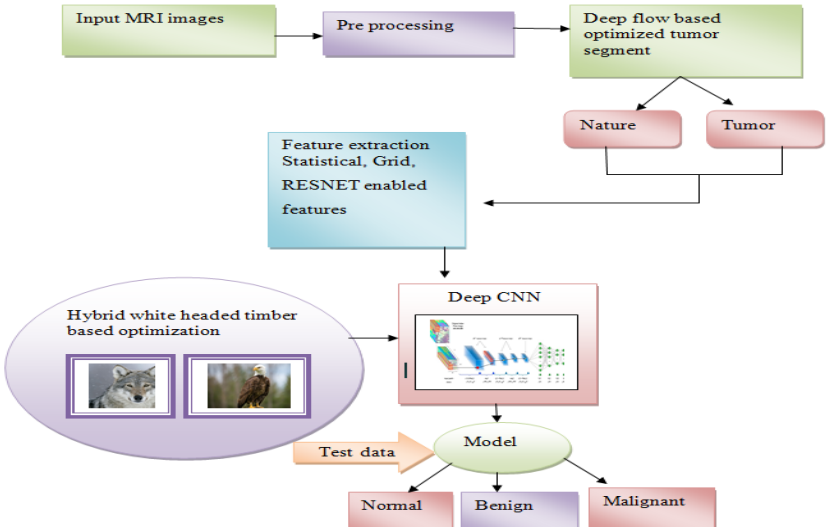


**Fig 1**: Block diagram representation of brain tumor prediction

**2.1 Input:**

The input for the brain tumor prediction model is collect from the d1 [16] and d2 [17] datasets, which are specified as follows:

$$R = R_1 + R_2$$

$$R = \sum_{i=1}^{g} R_c + \sum_{j=1}^{h} R_d \quad (1)$$

**2.2 Preprocessing:**

This work uses NLM for image denoising, aiming to find related patterns or textures by examining non-local portions of the image. NLM uses relativity between distant pixels, unlike local smoothing techniques. The noise is additive Gaussian noise, describing a discrete noisy image.

$$m(t) = f(t) + p(t) \quad (2)$$

Where, the observed value is represented as $q_t$, the original value is represented as $f(t)$, and the Gaussian noise is denoted as $p(t)$, and $t$ is the pixel index in the set, it is $D$.

$$NL(t) = \sum_{k \in \Omega} y(t,k) q(k) \quad (3)$$

Where $\Omega$ represents the window used to find similar pixels. The similarity between the pixels $t$ and $k$ determines the weights $\{y(t,k)\}_k$, which satisfy $0 \le y \le 1$ and $\sum_k y(t,k) = 1$. The Euclidean distance between the two blocks is frequently used to measure the similarity, which is respectively centered at the $t^{th}$ and the $k^{th}$ pixel, such that

$$y(t,k) = \frac{1}{b(t)} a^{\frac{-\|m(S_t) - m(S_k)\|_2^2}{i^2}} \quad (4)$$

**2.3 Deep flow based optimized tumor segmentation:**

BT detection classifies tumor forms and uses BT segmentation to locate malignant brain tissues and automatically label them. This technique aids in estimating tumor volume and identifying patient-specific features for diagnosis and therapy planning. The white-headed timber technique is used in this research for segmentation.

**2.4 Feature extraction:**

The feature extraction method extracts visual information from images, enabling decision-making similar to pattern recognition by normalizing the raw image.

***2.4.1 Grid based features:***

Grid-based features offer a structured representation of images, enabling classifiers to analyze specific regions and their characteristics for more precise tumor prediction and analysis.

***2.4.2 LDP:*** LDP, a texture descriptor, uses intensity changes to encrypt micro-level image data. It computes edge responses for each pixel in eight directions, encoding relative changes into binary code. The 8-bit LDP codes are only constructed for the $f$ most prominent directions because the outcome values are not equally relevant in all directions. Only the top responses are set to 1, while the rest of the $(8-f)$ responses are set to 0. LDP codes are generated by

$$LDP_f = \sum_{j=0}^{7} h(u_j - u_f) \times 2^j, h(i) = \begin{cases} 1, & if\ i \geq 0 \\ 0 & if\ i < 0 \end{cases} \quad \textbf{(5)}$$

The terms $u_j$ and $u_f$ stand for the edge response in the $j^{th}$ and $f^{th}$ most significant directional responses, respectively.

***2.4.3 LOOP:*** The LOOP texture descriptor represents local patterns in images using binary codes. It addresses orientation dependency and the LDP descriptor's 1 bit limit. It combines LDP and LBP strength to apply weights and identify intensity differences.

The eight direction's intensity variations are first determined by computing the eight Kirsch mask responses $(u_j, j = 0,1,.....7)$, which correspond to the pixels with intensities $(t_j = 0,1,.....7)$. Next, based on the magnitude value's rank $u_j$, each pixel is given a weight $q_j$. The following formula is used to calculate a LOOP code in the third stage, the center pixel $(i_s, a_s)$:

$$LOOP(i_s, c_s) = \sum_{j=0}^{7} 8(t_j - t_s) \times 2^{qj}, e(i) = \begin{cases} 1, & if\ i \geq 0 \\ 0, & if\ i < 0 \end{cases} \quad \textbf{(6)}$$

Where, the grayscale value of the central pixel is indicated in bytes. This research also considers the frequency distribution of these codes across the entire image, along with the LOOP features created by 3X3 image patches.2

***2.4.4 RESNET enabled method based features:***

ResNet-101 uses residual blocks with multiple Convolutional layers, batch normalization, and ReLU activation functions to learn residual functions. Its deep design and fine-grained features improve accuracy and reliability in predicting brain tumor patterns compared to shallower networks.

**2.5 Working of deep CNN classifier in brain tumor prediction:**

A deep CNN classifier uses convolutional and pooling operations to extract valuable information from brain tumor images. It determines if an image contains a tumor by feeding these features into linked layers for classification.

***a) Convolutional layer:***

The initial Convolutional Layer (CNN) is the crucial component of CNN, extracting low-level characteristics from input data, with subsequent layers used for complex features.

$$\hat{R} = \sum_{s} R_s \otimes T_{sb} + f_b \quad (7)$$

Where, $T_{s,b}$ represents the Convolutional kernel, $f_b$ stands for the bias, $R_s$ denotes the $s^{th}$ input feature map, $\hat{R}_b$ indicates the $b^{th}$ output feature map, and $\otimes$ stands for the 2-D convolution technique. In CNNs, both $T_{s,b}\ and\ f_b$ are the learnable parameters.

***b) Non linearity features:***

The second layer of the model represents the layer of non-linearity. The nonlinear component was added to CNN to enhance its fitting skills. This is accomplished by using activation processes like Sigmoid, ReLU, leaky ReLU, ELU, etc. The ReLU function is the most popular because to its ease of use and low computational requirements. It is expressed using the equation (Equation 15), with $q$ serving as the input value.

$$R(q) = \begin{cases} q, & if\ q > 0 \\ 0, & otherwise \end{cases} \quad (8)$$

***c) Pooling Layer:***

The Convolutional layer, despite its significant characteristics, can be over-fitted and slow in training, hence it employs down sampling to reduce parameters and compress the image.

$$M_c^p = t_b\left(H_c^p\right) \quad (9)$$

The pooling operation is depicted in Equation (16), where $t_b(.)$ indicates the type of pooling operation and $M_c^p$ represents the pooled feature-map of the $c^{th}$ layer for the $p^{th}$ input feature-map $H_c^p$. A group of features that are robust to minor translational shifts and distortions are extracted using the pooling method. By minimizing over fitting, shrinking the feature-map to an invariant feature set not only reduces network complexity but also promotes generalization.

***d) Fully connected layer:***

The FC layer at the network's edge enhances the performance of the layer below it, determining the number of classes based on the outcome.

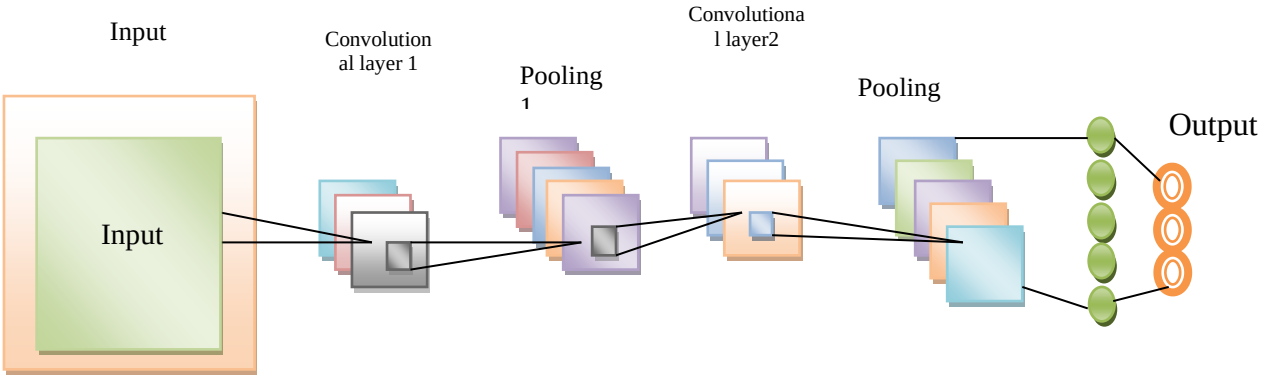


**Fig 2:** Deep CNN classifier model architecture

**2.6. Proposed white headed timber optimization:**

The WHT optimization in deep CNN classifiers allows fine-tuning of parameters, weights, and biases. It is often created through hybridization of bald eagle and grey wolf optimizations. Grey wolves face time complexities due to group hunting, while white head eagles swoop prey immediately, reducing complexity. Position update for grey wolves occurs through the swooping strategy.

***2.6.1 Motivation:***

Canis lupus served as inspiration for the recently developed Grey Wolf Optimizer (GWO), which mimics grey wolves social dominance and hunting techniques. The GWO approach uses the term alpha ( $\rho$ ) to refer to the population-wide fittest solution. The beta ( $\sigma$ ) and delta ( $\tau$ ), respectively, stand for the second- and third-best solutions. Omega ( $\lambda$ ) is supposed to represent the remaining population members.

Numerous organisms in nature inspire researchers to recreate and imitate their unique navigational, social, and hunting techniques. One of the top predators on the food chain, eagles is thought to be scavengers who prefer to consume simple or protein-rich food.

***a) Initialization:***

The three best solutions are given three random positions in the search space when the algorithm begins. The best solutions are indicated by $\rho, \sigma \, and \, \tau$ , while the remaining solutions are abbreviated as $\lambda$ .The $\lambda$ solutions follow the $\rho, \sigma \, and \, \tau$ timbers to incrementally increase their positions.

***b) Selection space:***

A mathematical equation depicts the activity of white-headed eagles in the selected space as they locate and choose the optimal place for food availability inside the search space.

$$Q_{new}, m = Q_r + \delta * s\left(Q_{mean} - Q_m\right) \tag{10}$$

Where, $s$ is a random number with a value between 0 and 1, and $\delta$ is a parameter for regulating positional changes that takes values between 1.5 and 2. White-headed eagles use the information from the previous stage to help them choose a place during the selection stage. A different search location is chosen at random by the eagle, but it is close to the first one. The search area known as $Q_r$ is the one that white-headed eagles have chosen right now based on the best result they found during their previous search. All locations in nearby area of the pre-selected search zone are randomly searched by eagles. Meanwhile, $Q_{mean}$ states that these eagles have absorbed all of the information from the prior locations. The present movement of the white-headed eagle is calculated by $\delta$ times the earlier data that was randomly searched. All search points are changed at random by this method.

***c) Search space:***

The white-headed eagle searches for prey in the chosen search space during the search stage. To speed up their search, they travel in different directions within a spiral space. According to mathematics, the ideal swoop position is as follows:

$$Q_{m,new} = Q_m + g(m) * \left(Q_m - Q_{m+1}\right) + f(m) * \left(Q_m - Q_{mean}\right) \tag{11}$$

$$f(m) = \frac{fs(m)}{\max\left(|fs|\right)}, g(m) = \frac{gs(m)}{\max\left(|gs|\right)} \quad \text{(u)}$$

The parameter $Y$ determines how many search cycles there will be whose range is 0.5 to 2, and the parameter

$u$ determines the corner between-point searches in the central point, whose range is 5 to 10. The criteria for the change in the spiral shape are represented by $u$ and $Y$.

## 3. Result and discussions:

The performance of the deep CNN model is evaluated in the prediction of brain cancers and contrasted with other methods.

### 3.1 *Brats 2019 [d1] & Brats 2020 [d2]*

The main objective of BraTS has always been the assessment of state-of-the-art techniques for the segmentation of brain tumors in multimodal MRI data. Pre-operative MRI scans from a number of institutions are used in BraTS 2020, which mainly concentrates on the segmentation (Task 1) of gliomas, which are intrinsically different brain cancers. In addition to focusing on the prediction of patient overall survival (Task 2) and the differentiation between false progression and actual tumor recurrence (Task 3), BraTS'20 also uses integrated analyses of radiomic features and ML algorithms to assess the clinical relevance of this segmentation task. Finally, Task 4 of BraTS'20 intends to evaluate the algorithmic uncertainty of tumor segmentation.

### 3.2 Experimental result:

Figure 3 illustrates the WHO-based deep CNN model with a number of features. Figure 3a shows the original input image; Figures 3b and 3c show the grid extracted image and the LDP image, Figures 3d and 3e show the loop extracted image, and the segmented output image and figure 3e shows the RESNET 101 extracted image.

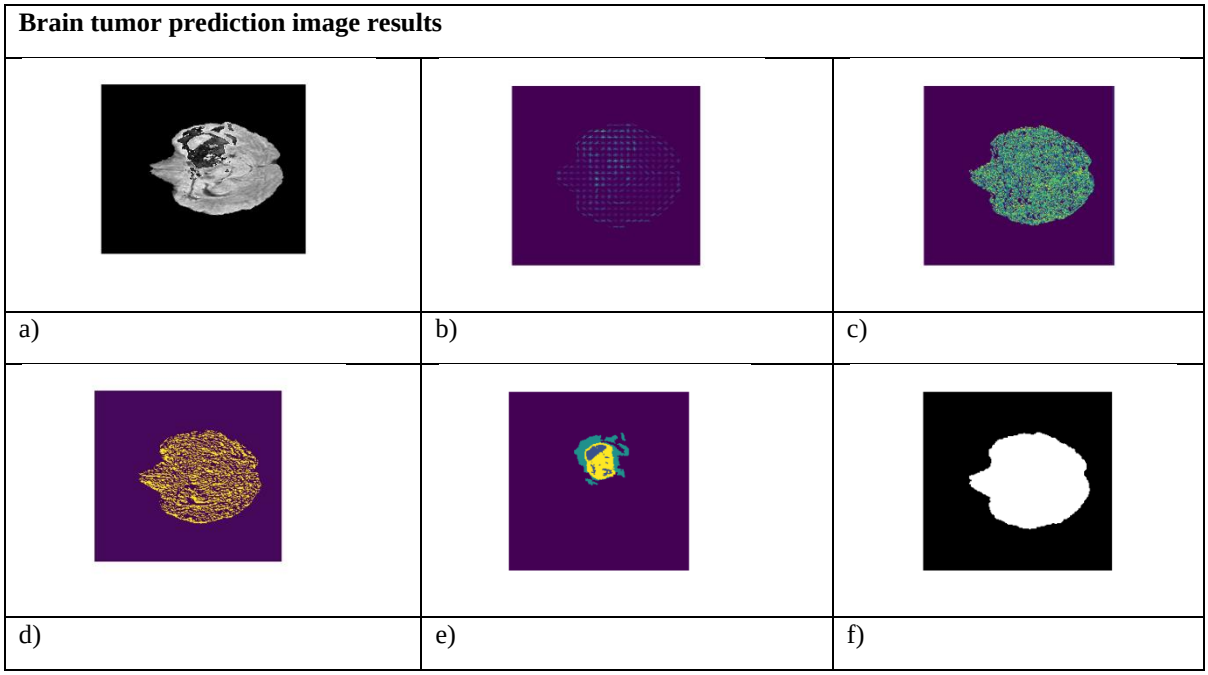


**Fig 3:** Experimental result obtained using WHO based deep CNN model

### 3.3 Comparative discussion:

Comparative analysis is performing through comparative analysis to demonstrate the superiority of the D8 models over the existing model. Although the TP and k-fold were consider using database 1, the metrics for D1 and D2 results were obtained during k-fold 10 for d1 98.37%, 98.31%, and 98.88% and d2 are 97.74%, 98.53%, and 99.15%. The following expressions are processed by the database, as depicted in tables 1.

**Table 1:** Comparative discussion table during K-fold 10

| | K-fold 10 | | | | | |
|---|---|---|---|---|---|---|
| | D1 | | | D2 | | |
| Models | Acc | Sen | Spe | Acc | Sen | Spe |
| SGD | 90.6 | 90.33 | 97.52 | 90.7 | 90.4 | 93.3 |
| LGBM | 91.3 | 91.05 | 97.64 | 92.2 | 91.39 | 95.31 |
| DBN | 91.99 | 91.76 | 97.76 | 93.12 | 92.4 | 96.13 |
| DNN | 92.69 | 92.48 | 97.89 | 93.99 | 93.29 | 96.98 |
| Deep CNN | 93.39 | 93.2 | 98.01 | 94.75 | 93.97 | 97.84 |
| BEO Deep CNN | 94.1 | 93.92 | 98.13 | 95.48 | 94.61 | 98.66 |

| | | | | | | |
|---|---|---|---|---|---|---|
| GWO Deep CNN | 94.8 | 94.65 | 98.26 | 95.93 | 95.25 | 98.9 |
| WHT based Deep CNN | 98.37 | 98.31 | 98.88 | 97.74 | 98.53 | 99.15 |

## 4. Conclusion

In this research develop a WHT based deep CNN model for predict brain cancers using MRI scans. The d1 and d2 is the initial source of the input for the MRI images. It next passes through the pre-processing stage, where the image's quality is assessed and any extraneous indicators are eliminated. After that this pre-processed image is passing through the segmentation stage the image is segmented based on the optimized deep flow. The portions of the pre-processed MRI images were clustered together that are representative of the same object class in terms of the type of tumour and nature. After that, the segmented images forward to the feature extraction stage, where features were taken from the MRI image's detailed representation of the brain. Additionally, the feature-extracted image is passed through the suggested optimised deep CNN classifier, which classifies and labels clusters of pixels or vectors within an image. The hyper parameters are then fine-tuned using the white-headed-timber based optimisation, which makes use of the characteristics of white headed eagle Optimization and timber Optimization. Although the TP and k-fold were consider using database 1, the acc, sen, and spe for D1 and D2 were achieved at 98.37%, 98.31%, and 98.88% correspondingly. For d2, the values were 97.74%, 98.53%, and 99.15%. Similar results were obtained during k-fold 10 for d1 96.93%, 96.63%, and 97.42% and d2 are 97.74%, 96.53%, and 98.95%.

## References


[1] Irmak, E., "Multi-classification of brain tumor MRI images using deep convolution neural network with the fully optimized framework," Iranian Journal of Science and Technology, Transactions of Electrical Engineering, vol.45,no.3, pp.1015-1036, 2021. Available from: https://link.springer.com/article/10.1007/s40998-021-00426-9

[2] Hashemzehi, R., Mahdavi, S.J.S., Kheirabadi, M. and Kamel, S.R., "Detection of brain tumors from MRI images base on deep learning using hybrid model CNN and NADE,"biocybernetics and biomedical engineering,vol. 40,no.3, pp.1225-1232, 2020. Available from: http://dx.doi.org/10.1016/j.bbe.2020.06.001

[3] Sharif, M.I., Li, J.P., Khan, M.A. and Saleem, M.A., "Active deep neural network features selection for segmentation and recognition of brain tumors using MRI images," Pattern Recognition Letters, vol.129, pp.181-189, 2020. Available from: https://www.sciencedirect.com/science/article/abs/pii/S0167865519303411

[4] Sharif, M.I., Li, J.P., Amin, J. and Sharif, A., "An improved framework for brain tumor analysis using MRI based on YOLOv2 and convolution neural network," Complex & Intelligent Systems, vol.7,no.4, pp.2023-2036, 2021. Available from: https://link.springer.com/article/10.1007/s40747-021-00310-3

[5] Sharif, M., Amin, J., Raza, M., Yasmin, M. and Satapathy, S.C., "An integrated design of particle swarm optimization (PSO) with a fusion of features for detection of brain tumor," Pattern Recognition Letters, vol.129, pp.150-157, 2020. Available from: http://dx.doi.org/10.1016/j.patrec.2019.11.017

[6] Rammurthy, D. and Mahesh, P.K., "Whale Harris hawks optimization based deep learning classifier for brain tumor detection using MRI images," Journal of King Saud University-Computer and Information Sciences, 2020. Available from: http://dx.doi.org/10.1016/j.jksuci.2020.08.006

[7] Bhargavi, K. and Mani, J.J., "Early Detection of Brain Tumor and Classification of MRI Images Using Convolution Neural Networks," Springer, Singapore, In Innovations in Computer Science and Engineering, pp. 427-436, 2019. Available from: https://link.springer.com/chapter/10.1007/978-981-13-7082-3_49

[8] Ferahtia, S., Rezk, H., Abdelkareem, M.A. and Olabi, A.G., "Optimal techno-economic energy management strategy for building's microgrids based bald eagle search optimization algorithm," Applied Energy, vol.306, pp.118069, 2022. Available from: https://doi.org/10.1016/j.energy.2022.123447

[9] Mirjalili, S., Mirjalili, S.M. and Lewis, A., "Grey wolf optimizer. Advances in engineering software,"vol.69, pp.46-61, 2014. Available from: http://dx.doi.org/10.1016/j.advengsoft.2013.12.007

[10] Gower, Robert Mansel, Nicolas Loizou, Xun Qian, Alibek Sailanbayev, Egor Shulgin, and Peter Richtárik. "SGD: General analysis and improved rates." In International conference on machine learning, pp. 5200-5209. PMLR, 2019. Available from: https://doi.org/10.48550/arXiv.1901.09401

[11] Aziz, Rabia Musheer, Mohammed Farhan Baluch, Sarthak Patel, and Abdul Hamid Ganie. "LGBM: a machine learning approach for Ethereum fraud detection." International Journal of Information Technology 14, no. 7 (2022): 3321-3331. Available

from: http://dx.doi.org/10.1007/s41870-022-00864-6

[12] Yang, Ying. "Medical multimedia big data analysis modeling based on DBN algorithm." IEEE Access 8 (2020): 16350-16361. Available from: https://doi.org/10.1109/ACCESS.2020.2967075

[13] Mittal, Sparsh. "A survey on modeling and improving reliability of DNN algorithms and accelerators." Journal of Systems Architecture 104 (2020): 101689. Available from: https://doi.org/10.1016/j.sysarc.2019.101689

[14] Sayed, Gehad Ismail, Mona M. Soliman, and Aboul Ella Hassanien. "A novel melanoma prediction model for imbalanced data using optimized SqueezeNet by bald eagle search optimization." Computers in biology and medicine 136 (2021): 104712. Available from: https://doi.org/10.1016/j.compbiomed.2021.104712

[15] Kumar, Abhishek, SwarnAvinash Kumar, Vishal Dutt, Ashutosh Kumar Dubey, and Vicente García-Díaz. "IoT-based ECG monitoring for arrhythmia classification using Coyote Grey Wolf optimization-based deep learning CNN classifier." Biomedical Signal Processing and Control 76 (2022): 103638. Available from: https://doi.org/10.1016/j.bspc.2022.103638

[16] BRATS 2019 dataset Available from: https://www.kaggle.com/datasets/aryashah2k/brain-tumor-segmentation-brats-2019

[17] BRATS 2020 dataset Available from: https://www.kaggle.com/datasets/awsaf49/brats2020-training-data.